Morphological equilibration of a corrugated crystalline surface

M. Ozdemir and A. Zangwill
School of Physics, Georgia Institute of Technology, Atlanta, Georgia 30332-0432
(Received 17 April 1990)

We study the flattening of a corrugated crystal surface for the case when mass transport is driven by surface diffusion and the temperature is well below the roughening temperature of the equilibrium facet. For the considered geometry, the problem is one dimensional and the surface morphology consists of a collection of terraces separated by straight, parallel steps. In this situation, the kinetics is driven by step-step interactions alone. We obtain separated variable (shape-preserving) solutions to both the differential equation of motion for the surface profile $z(x,t)$ and the discrete equations of motion for individual terraces' widths $l_n(t)$. Numerical solutions of these equations demonstrate that the analytic solution well describes the kinetics in the latter case. As morphological equilibration proceeds, we find that $z(x,t)\sim t^{-1}$ and that $l_n(t)\sim t^{1/5}$ or $l_n(t)\sim t^{1/4}$ for the cases of diffusion-limited or step-attachment-limited step propagation, respectively. These predictions are amenable to direct experimental tests.

I. INTRODUCTION

This paper is concerned with morphological changes which accompany diffusive mass transport on crystal surfaces. Examples of this phenomenon arise in a number of different contexts. For example, highly perfect single-crystal growth by, e.g., molecular-beam epitaxy (MBE) or vapor-phase epitaxy (VPE) occurs only when the substrate temperature is held within a fairly narrow range.[1,2] In both cases, the temperature must be low enough to suppress the deleterious effects of impurity incorporation and bulk interdiffusion yet high enough to guarantee smooth layer completion and avoid interface roughness. Generally speaking, the experimental trend is toward lower substrate temperatures coupled with deposition interruption techniques[3,4] which delay the arrival of new species in order to increase the efficacy of interface smoothing by surface diffusion. By necessity, attempts to optimize this procedure have been entirely empirical since the construction of a general theory of morphological evolution during epitaxial growth under typical experimental conditions is a difficult and incompletely solved problem.[5–8] This is so because one must couple a realistic account of mass transport (deposition and diffusion) with the "typical" surface morphology one encounters[9] in interesting cases: a distribution of islands (of various sizes and heights) distributed atop the terraces of a vicinal surface.

Clearly, the basic problem of describing this complex morphology remains even if, as in some recent experiments,[10–12] we focus on the extreme case where the incident flux is arrested and one considers only the smoothing of the surface, i.e., the approach to morphological equilibration. However, if we instead restrict ourselves to a much *simpler* surface topography, e.g., a one-dimensional periodic corrugation, not only does the problem become tractable, but the kinetics of thermal annealing becomes directly relevant to recent discussions of surface reconstruction,[13] thermal roughening,[14] and the stability of semiconductor heterostructures.[15,16] Accordingly, this case is the subject of the present paper.

As it happens, the smoothing of a corrugated surface by surface diffusion was examined by Mullins[17,18] 30 years ago. Among other things, he showed that measurements of the rate of capillary-induced flattening of a sinusoidally rumpled surface could be used to extract surface diffusion constants. This suggestion was pursued soon thereafter[19] and such studies continue to the present day using lithographically prepared surfaces.[20,21] In some cases, such corrugations retain their sinusoidal shape as the perturbation amplitude decreases while, in other cases, distinct facets appear. Unfortunately, Mullins's analysis is not applicable to the latter cases because his theory presumes that all surface properties are smooth functions of crystallographic orientation, whereas facets arise[22,23] precisely from the existence of nonanalytic, cusped minima at particular angular orientations $\hat{\mathbf{n}}$ of the anisotropic surface tension $\gamma(\hat{\mathbf{n}})$. The same remark applies to the island and step morphology noted above in connection with typical epitaxial growth conditions.

Apart from a very early study by Geguzin and Ovcharenko[24] and some later work by Martin and Perraillon,[25] there appear to have been no serious attempts to generalize Mullins's theory to the case of a faceted crystal until very recently,[26] most particularly by Villain and co-workers.[14,27–30] Technically, one requires an analysis valid below the so-called *roughening temperature*[31,23] of the facets in question. The elucidation of the appropriate anisotropic surface thermodynamics is also of rather recent vintage.[32,33] Up until now, a satisfactory analysis of morphological equilibration by surface diffusion below T_R has been achieved only for the case of a multilevel surface composed of a collection of circular islands of various sizes on a flat surface. In this situation (directly relevant to the simplest polynuclear birth-and-spread models[34] of nucleation-dominated crystal growth) an essential simplification arises because each island spontaneously shrinks in radius in order to reduce its

(one-dimensional) line energy. But this driving force for surface smoothing *vanishes* for the case of one-dimensional surface profiles with straight, parallel terrace edges such as the sinusoidally corrugated surfaces of interest here. In this case, step-step interactions drive morphological evolution[25] and no complete theory is yet available. Monte Carlo simulation techniques have been brought to bear on the problem,[35,36] but these studies have been hampered by the extremely slow kinetics of surface diffusion.

In this work we present a complete analysis of the decay of periodic one-dimensional corrugations on a crystal surface by surface diffusion for the case when the final equilibrium corresponds to a single flat facet. By a combination of analytic and numerical techniques applied to appropriate discrete and continuum equations of motion we are able to study the motion of both individual steps and the envelope of the surface profile. We confirm a number of previous predictions[14,37] and make several new predictions which should be directly testable by experiment. The plan of the paper is as follows. In Sec. II, we review Mullins's theory of morphological equilibration valid for $T > T_R$ and complete Villain's extension of the same analysis to the case when $T < T_R$. Section III is devoted to the derivation of a more exact formulation of the problem when $T < T_R$ in terms of the motion of terrace edges. The resulting equations are solved and compared with the continuum theory in Sec. IV. Sections V and VI contain a discussion and summary, respectively.

II. CONTINUUM THEORY

In this section we treat the surface profile in a macroscopic continuum approximation[17,18] so that the instantaneous shape of the one-dimensional surface can be described by a height function $z(x,t)$. If mass transport occurs *only* by surface diffusion, the time variation of this quantity satisfies a continuity equation

$$\frac{\partial z}{\partial t} = -\Omega \frac{\partial j}{\partial x} , \tag{1}$$

where Ω is the atomic volume of the diffusing species and the surface current $j(x,t)$ is given by Fick's law as

$$j = -\frac{\nu D_S}{kT} \frac{\partial \mu}{\partial x} . \tag{2}$$

In this expression, ν is the areal density of diffusing species, D_S is the surface diffusion constant, and $\mu(x,t)$ is the spatially varying chemical potential of the adsorbed species. Note that, in writing (1) and (2), we have implicitly made a small-slope approximation since the spatial derivatives in these formulas actually should be taken with respect to the arc length of the curve $z(x,t)$. Finally, as first shown by Herring,[38] the surface chemical potential is given by[18]

$$\mu = -\Omega \frac{\partial}{\partial x} \left[\frac{\partial G}{\partial z_x} \right] , \tag{3}$$

where $z_x \equiv \partial z/\partial x$, and G is the surface tension per unit *projected* surface area,

$$G(z_x) = \gamma(z_x)(1+z_x^2)^{1/2} . \tag{4}$$

The notation is meant to indicate that, in the small-slope approximation, it will be sufficient to expand $\gamma(\hat{\mathbf{n}})$ and hence G in powers of z_x.

To proceed, we require explicit expressions for the surface energy. When $T > T_R$, G is an analytic function of z_x (Refs. 14, 18, and 23) in the vicinity of its relative minima. Therefore, taking account of symmetry, the appropriate expansion is

$$G = G_0 + \tfrac{1}{2} G_2 z_x^2 + \tfrac{1}{4} G_4 z_x^4 + \cdots . \tag{5}$$

Combining all the foregoing, we obtain Mullins's kinetic equation,

$$\frac{\partial z}{\partial t} = -B_1 \frac{\partial^4 z}{\partial x^4} , \tag{6}$$

where $B_1 = \nu \Omega^2 G_2 D_S / kT$ is an overall (positive) kinetic coefficient. By separation of variables, one immediately finds a *shape-preserving* solution:[17,18]

$$z(x,t) = z_0 \sin(kx) \exp(-B_1 k^4 t) . \tag{7}$$

Moreover, because the kinetic equation (6) is *linear,* the strong wave-vector dependence in the exponential implies that *any* periodic surface perturbation with repeat distance $2L = 2\pi/k$ rapidly approaches the above solution because the amplitudes of all higher Fourier components quickly decay to zero.

When $T < T_R$, (5) is no longer applicable since, as noted earlier, $\gamma(\hat{\mathbf{n}})$ exhibits cusp singularities. Current lattice models[31] predict that the appropriate replacement is

$$G = G_0 + G_1 |z_x| + \tfrac{1}{3} G_3 |z_x|^3 + \cdots . \tag{8}$$

The absence of a quadratic term in this expansion is not obvious and (when confronted with experiments on equilibrium crystal shape) by no means universally accepted.[39,40] Moreover, if (8) is inserted naively into (3), one obtains a δ function for the chemical potential when $z_x = 0$. By replacing this δ function with an analytic, yet sharply peaked, function and solving a generalized version of (6) numerically, Preuss *et al.*[41] obtained reasonable agreement with their experimental annealing data. But, as pointed out by Rettori and Villain,[14] the chemical potential cannot be singular and a more detailed analysis is required.[14,33] The appropriate expression turns out to involve only the last term in (8):

$$\mu = -2 G_3 \Omega |z_x| z_{xx} . \tag{9}$$

Combining this with (1) and (2) leads to Villain's equation of motion:[29]

$$\frac{\partial z}{\partial t} = -B_2 \frac{\partial^2}{\partial x^2} (|z_x| z_{xx}) , \tag{10}$$

where $B_2 = 2\nu \Omega^2 G_3 D_S / kT$.

By analogy with the earlier discussion valid for $T > T_R$, let us seek a shape-preserving solution by separation of variables. Setting $z(x,t) = u(x) w(t)$, and assuming that $w(t) > 0$, one finds

$$\frac{dw}{dt} = -\lambda w^2 \tag{11}$$

and

$$B_2 \frac{d^2}{dx^2}(|u_x|u_{xx}) = \lambda u \ , \tag{12}$$

where λ is a (positive) separation constant. Equation (11) is immediately integrated so that

$$z(x,t) = \frac{u(x)}{1+\lambda t} \ , \tag{13}$$

which, at least for this shape-preserving solution, confirms a speculation of Villain[37] regarding the time dependence. We have been unable to solve (12) exactly analytically. Accordingly, Fig. 1 illustrates a numerical solution of this equation (for a particular value of λ and periodic boundary conditions on an interval L) compared to a sinusoid of the same amplitude. Although the two curves are similar, $u(x)$ is *not* analytic near its extrema. This can be seen by seeking a solution to (12) in the immediate vicinity of, say, a local maxima $u_0(x_0)$. The result is

$$u(x) = u_0 - \alpha|x-x_0|^{3/2} + \frac{2}{63}\frac{\lambda u_0}{\alpha B_2}|x-x_0|^{7/2} + \cdots \ , \tag{14}$$

where α is a positive constant which depends only on u_0 and L. The first term (previously obtained by Lançon and Villain[29]) is the result one obtains near an *equilibrium* facet edge if (8) is valid.[31] The second term reminds us that λ actually parametrizes an entire family of solutions to (12). As it happens, our numerical studies show that the dependence of $u(x)$ on λ is extraordinarily small (on the scale of Fig. 1), so that the curve depicted there is, effectively, *the* shape-preserving solution. Unfortunately, because (10) is *nonlinear* (so that superposition is not valid) this solution has no obvious relevance to the decay of an arbitrary initial corrugation.

To study this more general question, we have integrated (10) numerically for a wide class of periodic starting surfaces. The sequence of curves in Fig. 2 illustrates the time evolution for the case of a sinusoidal initial profile. Apparently, the profile continuously deforms as flattening proceeds with no special status afforded to the shape-preserving solution. On the other hand, the time dependence of the profile amplitude *does* appear to follow (13) rather well (Fig. 3). Such a result would lend support to the suggestion[37] that this temporal behavior has a more general origin than as part of a shape-preserving solution. Be that as it may, a least-squares fit clearly reveals small but systematic deviations from $z^{-1} \sim t$ which persist even as numerical accuracy increases. Instead, our best data indicate that $z^{-1} \sim t^{1+\alpha}$ where $\alpha \simeq -0.05$. At present we have no explanation for this result.

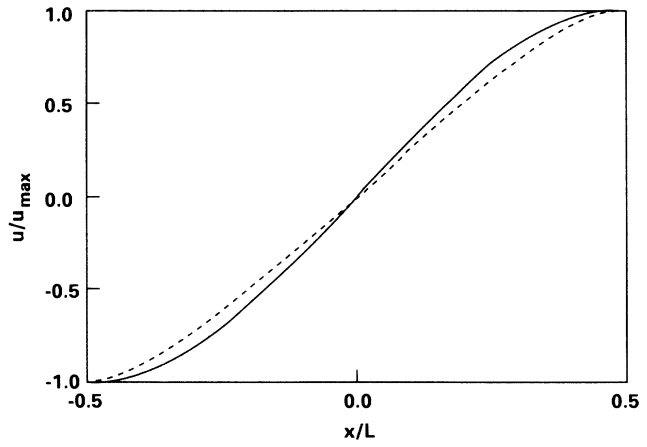

FIG. 1. Numerical solution of Eq. (12) (dashed curve) compared to a sinusoid (solid curve) of the same amplitude.

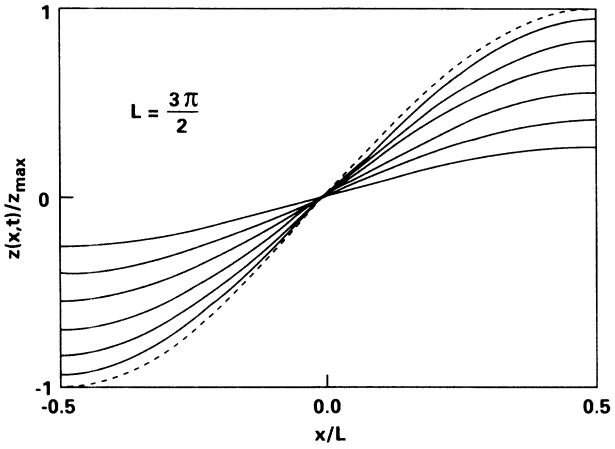

FIG. 2. Flattening of an initial sinusoidal profile (dashed curve) as determined by numerical solution of the continuum equation of motion (10).

III. THE KINETICS OF STEPS AND TERRACES

The treatment of the preceding section implicitly assumes that the crystal profile $z(x,t)$ is an analytic function almost everywhere. In fact, well below the roughening temperature, this is not true. Instead, a small-

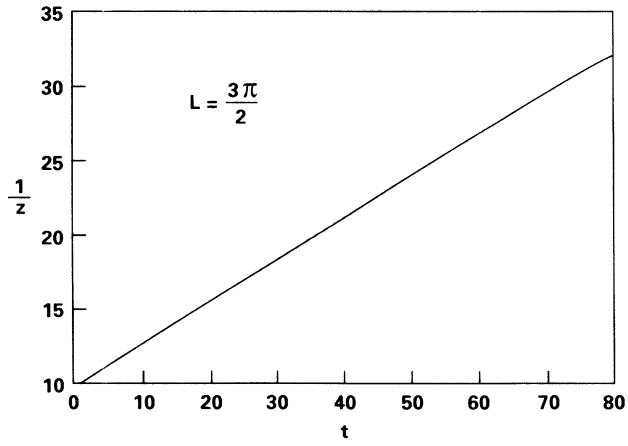

FIG. 3. Inverse profile amplitude vs time (both in arbitrary units) for the flattening sequence of Fig. 2.

amplitude shape perturbation about a single facet is best described as a collection of macroscopically flat terraces bounded by vertical steps. Thus, a detailed account of morphological evolution most correctly deals directly with the motion of individual steps. This approach has long been popular in connection with the theory of layer growth[42] and has, more recently, been applied to problems of equilibrium crystal shape,[43] step kinetics,[44] and morphological equilibration.[14,25–27] In this section we treat the decay of a one-dimensional periodic surface corrugation (Fig. 4) from this point of view.

As shown in Fig. 5, the net motion of any particular step involves a competition between two processes: (i) adatom diffusion toward the step from one of the two bounding terraces followed by attachment to a high-binding-energy site at the base of the step, and (ii) adatom detachment from the step edge followed by diffusion across one of the two bounding terraces. Our one-dimensional treatment (for which one should more properly speak of the motion of entire *rows* of atoms) will be correct at the macroscopic level so long as the terrace edges are above their (one-dimensional) roughening temperature. Moreover, in order to more closely describe the typical experimental situation,[45] we shall require neither that the diffusing species be in equilibrium with the terrace edges, nor that the nonequilibrium kinetic coefficients be equal on opposite sides of a step. Our general approach is similar in spirit to that adopted by Uwaha.[26]

Given the foregoing, the time evolution of the nth terrace edge (located at position x_n) can be described by a Ginzburg-Landau equation of the form

$$\Omega^{-1}\frac{dx_n}{dt}=-k_+\frac{\delta F^+}{\delta x_n}-k_-\frac{\delta F^-}{\delta x_n}\ , \tag{15}$$

where k_+ and k_- are the aforementioned kinetic coefficients and δF^+ and δF^- are the changes in the total free energy (per unit length of step) when nearby atoms adsorbed on the lower or upper bounding terrace, respectively, are transferred to a new atomic row at the base of the nth step. It is easy to see that

$$\delta F^+=\Omega^{-1}\int dx\ \delta x_n[\bar{\mu}_c-\bar{\mu}_n(x)]_+ +\int dx\ \delta G \tag{16}$$

and

$$\delta F^-=\Omega^{-1}\int dx\ \delta x_n[\bar{\mu}_c-\bar{\mu}_{n-1}(x)]_- +\int dx\ \delta G\ , \tag{17}$$

where $\bar{\mu}_c$ is the chemical potential of an atom bound to the crystal at the step edge, $\bar{\mu}_n(x)$ is the position-dependent chemical potential of an atom adsorbed on the nth terrace, and δG is the change in the projected surface tension (4). The subscripts on the square brackets indicate that the enclosed quantities are to be evaluated on the terrace in question at a point immediately adjacent to an up (+) or down (−) step.

To compute δG, note that the local profile slope is related to the step height h and the mean terrace width l by $|z_x|=h/l$, so that the linear term in (8) may be interpreted as a sum of individual step free energies, while the cubic term may be taken[46] to represent the total interaction energy between *pairs* of steps. Therefore, more precisely,

$$G=G_0+G_1|z_x|+\tfrac{1}{3}G_3\frac{h^3}{L}\sum_n\frac{1}{l_n^2}+\cdots\ , \tag{18}$$

where l_n denotes the actual width of the nth terrace and $L=\sum_n l_n$. This equation makes explicit the existence of an effective inverse-cube repulsive force between neighboring "like" steps, i.e., those which do not bound the terraces at the maxima and minima of the profile. This force arises in part from step-induced surface stress and strain[47,48] and in part from configurational entropy considerations.[49] For simplicity, we shall assume that there is *no* force acting between neighboring "unlike" steps.[50] Carrying out the virtual transfer of particles envisaged above, it is straightforward to compute that

$$\delta G=\tfrac{2}{3}G_3h^3\left(\frac{1}{l_n^3}-\frac{1}{l_{n-1}^3}\right)\frac{\delta x}{L}=\frac{\mu_n}{\Omega}\delta x\ , \tag{19}$$

which serves to define a chemical potential for steps.[14] Specifically, taking special account of those steps with "unlike" neighbors,

$$\mu_1=\frac{K}{l_1^3}\ ; \tag{20a}$$

$$\mu_n=K\left(\frac{1}{l_n^3}-\frac{1}{l_{n-1}^3}\right),\quad 1<n\le N\ ; \tag{20b}$$

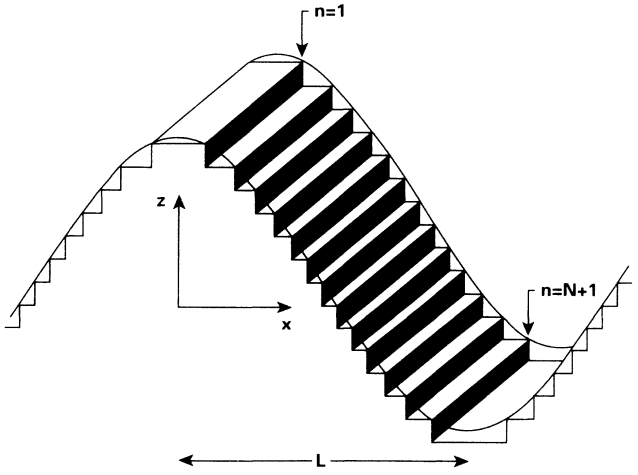

FIG. 4. Sinusoidally corrugated surface for $T<T_R$.

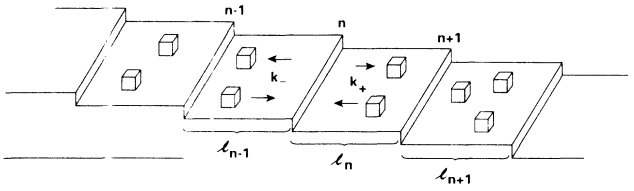

FIG. 5. Enlargement of Fig. 4 illustrating the labeling of steps and terraces and the definitions of $k_\pm$, the kinetic coefficients for adatom attachment or detachment to or from a step from or to the two bounding terraces.

$$\mu_{N+1}=-\frac{K}{l_N^3}\ ; \tag{20c}$$

where $K=\frac{2}{3}\Omega G_3 h^3/L$.

The equation of motion (15) then takes the form

$$\frac{dx_n}{dt}=k_+[\Delta\bar{\mu}_n(x)-\mu_n]_+ + k_-[\Delta\bar{\mu}_{n-1}(x)-\mu_n]_- = v_n^+ + v_n^- \ , \tag{21}$$

where $\Delta\bar{\mu}$ stands for the *negative* of the chemical potential difference in (16) or (17). On the other hand, one knows from textbook discussions[51,52] of diffusion problems with moving boundaries that mass conservation requires that

$$\frac{dx_n}{dt}=\bar{v}D_S\left[\left.\frac{dc_n}{dx}\right|_{x_n^+}-\left.\frac{dc_{n-1}}{dx}\right|_{x_n^-}\right]=v_n^+ + v_n^- \ , \tag{22}$$

where $c_n(x)$ is the concentration of diffusing species on the nth terrace and $\bar{v}=v^{-1}$. To make the connection between (21) and (22), we expand the chemical potential on any terrace about the equilibrium adsorbate concentration,

$$\Delta\bar{\mu}[c(x)]=\bar{\mu}(c_{\rm eq})+\frac{\partial\bar{\mu}}{\partial c}[c(x)-c_{\rm eq}]-\bar{\mu}_c = \frac{\partial\bar{\mu}}{\partial c}c(x)+\kappa \ , \tag{23}$$

so that, for example,

$$v_n^+=k_+\left[\frac{\partial\bar{\mu}}{\partial c}c_n(x)+\kappa-\mu_n\right]_+=\bar{v}D_S\left.\frac{dc_n}{dx}\right|_{x_n^+} \tag{24}$$

and

$$v_{n+1}^-=k_-\left[\frac{\partial\bar{\mu}}{\partial c}c_n(x)+\kappa-\mu_{n+1}\right]_-=-\bar{v}D_S\left.\frac{dc_n}{dx}\right|_{x_{n+1}^-} . \tag{25}$$

The right-hand sides of these two equations are precisely the boundary conditions required to compute $c_n(x)$ as a steady-state solution to the surface diffusion equation

$$\frac{\partial c_n}{\partial t}=D_S\frac{\partial^2 c_n}{\partial x^2}=0 \ . \tag{26}$$

Equation (26) is solved by

$$c_n(x)=a_n+b_n x, \quad x_n\le x\le x_{n+1} \tag{27}$$

with $b_0=b_{N+1}=0$ (by symmetry) and [upon application fo (24) and (25)]

$$b_n=\frac{\mu_{n+1}-\mu_n}{\bar{v}D_S(1/k_+ +1/k_-)+(\partial\bar{\mu}/\partial c)(x_{n+1}-x_n)} = \left[\frac{\partial\bar{\mu}}{\partial c}\right]^{-1}\frac{\mu_{n+1}-\mu_n}{d+l_n} \ . \tag{28}$$

In this equation, the terrace width $l_n=x_{n+1}-x_n$ and $d=\bar{v}D_S(k_+^{-1}+k_-^{-1})(\partial\mu/\partial c)^{-1}$. An expression similar to (28) can be derived for the a_n, but since [from (2), (23), and (27)] each b_n is directly proportional to the diffusive current across the nth terrace, only they are required to compute the step velocities

$$v_n=\bar{v}D_S(b_n-b_{n-1}) \tag{29}$$

and the equation of motion for the terrace widths,

$$\dot{l}_n(t)=\bar{v}D_S(b_{n+1}-2b_n+b_{n-1}) \ . \tag{30}$$

Equation (30) is the central result of this section.

IV. SOLUTION OF THE EQUATIONS OF MOTION

In this section we seek solutions to (30) with [combining (20) and (28)]

$$b_0=0 \ ; \tag{31a}$$

$$b_1=\frac{B_3}{d+l_1}\left[\frac{1}{l_2^3}-\frac{2}{l_1^3}\right] ; \tag{31b}$$

$$b_n=\frac{B_3}{d+l_n}\left[\frac{1}{l_{n+1}^3}-\frac{2}{l_n^3}+\frac{1}{l_{n-1}^3}\right], \quad 1<n<N \ ; \tag{31c}$$

$$b_N=\frac{B_3}{d+l_N}\left[-\frac{2}{l_N^3}+\frac{1}{l_{N-1}^3}\right] ; \tag{31d}$$

$$b_{N+1}=0 \ ; \tag{31e}$$

where $B_3=K/(\partial\bar{\mu}/\partial c)$. These are difference equations; but, to gain some insight, it is useful first to treat the step label n as a continuous variable and study the corresponding differential equation:

$$\dot{l}_n(t)=B_4\frac{\partial^2}{\partial n^2}\left[\left[\frac{1}{d+l_n}\right]\frac{\partial^2}{\partial n^2}\left[\frac{1}{l_n^3}\right]\right] . \tag{32}$$

Here, $B_4=\bar{v}D_S B_3$. Regretably, even this equation appears to be intractable. To make progress, note that the quantity d [defined below Eq. (28)] is a length which measures the relative importance of step-attachment kinetics ($k_\pm$) to surface diffusion (D_S) for our problem: "step-attachment-limited" motion corresponds to $d\gg l$, while "diffusion-limited" step propagation occurs when $d\ll l$. In what follows we will treat these two limiting cases separately and revisit the general case only at the end of this section. For the case of fast kinetics, our difference equations reduce to those written down (but not solved) previously by Rettori and Villain.[14]

Once again, we proceed by separation of variables. It is easy to verify that (32) is solved by

$$l_n(t)=A_n(5\lambda t+D)^{1/5} \ , \tag{33}$$

where $D=[l_n(0)/A_n]^5$ and

$$B_4\frac{d^2}{dn^2}\left[\frac{1}{A_n}\left[\frac{d^2}{dn^2}\frac{1}{A_n^3}\right]\right]=\lambda A_n \tag{34}$$

for the case of fast attachment kinetics ($d\to 0$) and

$$l_n(t)=A_n(4\lambda t+D)^{1/4} \ , \tag{35}$$

where now $D=[l_n(0)/A_n]^4$ and

$$\frac{B_4}{d}\frac{d^4}{dn^4}\left[\frac{1}{A_n^3}\right]=\lambda A_n \tag{36}$$

for the case of slow attachment kinetics ($d\to\infty$). Evidently, in both cases, the initial profile must satisfy

$$\frac{l_1(0)}{A_1}=\frac{l_2(0)}{A_2}=\cdots=\frac{l_n(0)}{A_N}\ . \tag{37}$$

This guarantees that the ratios $l_n(t)/A_n$ remain equal as evolution proceeds, i.e., that the solutions (33) and (35) are *shape preserving*. The separation constant λ (which must be positive in both cases) plays a different role here than in the analysis of Villain's equation. To see this, note that (33) and (34) are invariant under the replacement $A_n\to\lambda^{-1/5}A_n$ and (35) and (36) are invariant under the replacement $A_n\to\lambda^{-1/4}A_n$. Thus, a change in λ is equivalent to a uniform rescaling of the terrace widths and its value may be chosen for convenience. To simplify matters in what follows, we generally will choose $\lambda=\frac{1}{5}$ and $\frac{1}{4}$ for the cases of fast and slow kinetics, respectively.

It remains only to compute the A_n from (34) and (36). The (four) boundary conditions required to do so can be found from (30) and (31). However, there appears to be little reason to pursue this computation. Instead, we return to the full set of difference equations and (in each case) use the separated solution obtained from the corresponding differential equation as a trial *ansatz*. We find that these solutions exactly satisfy the discrete equations as well. More precisely, if (33) and (35) are substituted into (30), taking the appropriate limit in (31), respectively, a solution is obtained if the A_n satisfy

$$\lambda A_n=B_4(K_{n+1}-2K_n+K_{n-1})\ , \tag{38}$$

where

$$K_0=0\ ; \tag{39a}$$

$$K_1=\frac{1}{A_1}\left[\frac{1}{A_2^3}-\frac{2}{A_1^3}\right]\ ; \tag{39b}$$

$$K_n=\frac{1}{A_n}\left[\frac{1}{A_{n+1}^3}-\frac{2}{A_n^3}+\frac{1}{A_{n-1}^3}\right],\quad 1<n<N\ ; \tag{39c}$$

$$K_N=\frac{1}{A_N}\left[-\frac{2}{A_N^3}+\frac{1}{A_{N-1}^3}\right]\ ; \tag{39d}$$

$$K_{N+1}=0\ ; \tag{39e}$$

when $d\ll l_n$ and identical formulas when $d\gg l_n$, except that the prefactors to the expressions in large parentheses in (39) become d^{-1} everywhere.

We have solved these nonlinear difference equations numerically for various values of N, the total number of terraces in one half-period of the surface corrugation (Fig. 4). Surprisingly, the computed values of A_n for the case of fast kinetics ($d\ll l_n$) differ from those computed for the case of slow kinetics ($d\gg l_n$) by very nearly a *constant* for all values of n and N. This is illustrated in Fig. 6, where the computed values have been normalized to a common value (for each N) at $n=1$.

It is interesting to compare the shape-preserving solutions found here with those obtained in Sec. II. We have noted already that the separation constant λ does not parametrize a family of such curves as in the continuum limit. However, the "universal" $|x-x_0|^{3/2}$ behavior near local extrema *is* reproduced. In the step language, this translates to $A_n\sim|n-n_0|^{-1/3}$, where n_0 labels a step bounding one of the extrema (Fig. 7). As shown by Rettori and Villain,[14] this arises when the diffusive current across a terrace (our b_n) is very weak.

We can now address the question of morphological equilibration. Flattening occurs because all terraces widths expand according to (33) or (35) *except* those at local maxima and minima. No true "facets" ever form.[14] Instead, the terraces at the top and bottom of the corrugation wave shrink and eventually vanish as their bounding steps approach, collide, and annihilate. Upon annihilation, the number of steps decreases by two and the amplitude decreases accordingly. The process repeats until no steps remain. This scenario makes clear how the system rids itself of the excess free energy of individual steps [G_1 in (18)] despite the fact that the kinetic equations of motion (10) and (32) explicitly depend only on the step-step interaction strength G_3. As noted in the Sec. I, this behavior is peculiar to the one-dimensional geometry of an array of straight steps. Line-tension effects dominate whenever step-edge curvature is present.[14,26]

Observe that, if $d\gg l_n(0)$, a crossover from kinetic to diffusion-limited step motion may be expected as evolution proceeds. Although this transition will be reflected in a change in the time dependence of the terrace widths, there will be very little perceptible change in the profile shape due to the similarity of the two curves in Fig. 6.

The foregoing is correct, but incomplete. In particular, since the total number of steps, N, is a function of time, the $A_n(N)$ must be functions of time as well. To see the consequences of this, suppose a terrace system is shape

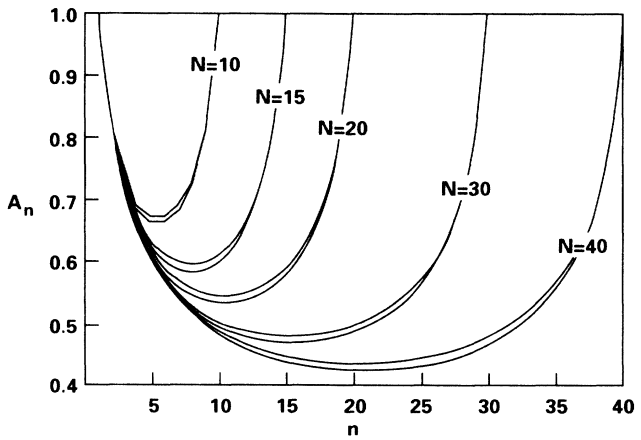

FIG. 6. Solutions to Eqs. (34) and (36) for various values of N. Although plotted as continuous curves, the A_n are, in fact, only defined at integer values of n.

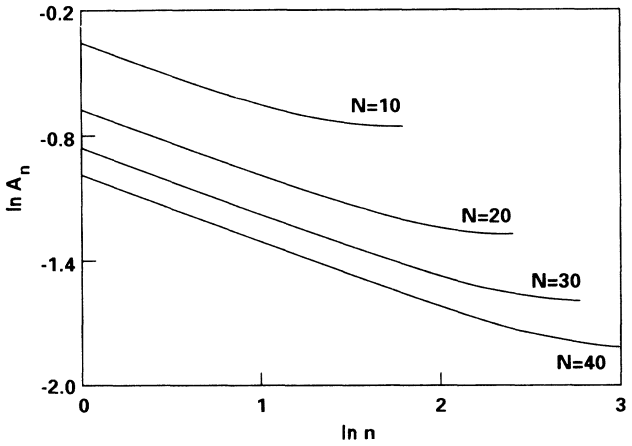

FIG. 7. Demonstration that the A_n of Fig. 6 reproduce the extremal behavior of the shape-preserving solution (14) to the continuum equation of motion (10). The straight-line segments have a slope of $-1/3$.

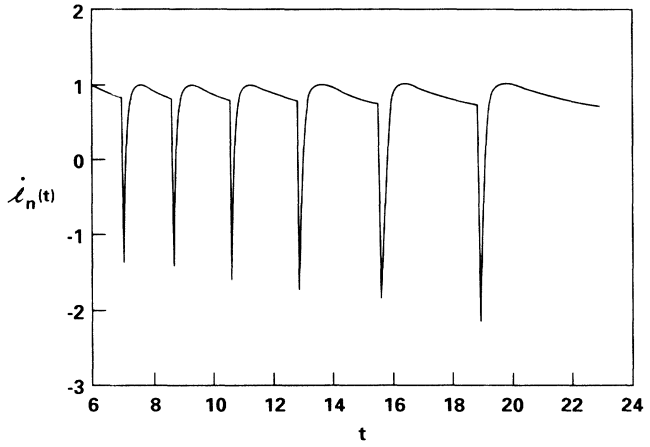

FIG. 9. Velocity of a "typical" terrace width for a time interval of morphological evolution during which several steps annihilate. Both scales are in arbitrary units.

preserving for some value of N. Immediately after annihilation of the top and bottom terraces occurs, the surface profile does not, indeed *cannot,* possess the correct separated solution shape for a system of $N-2$ steps. There then appears to be no reason to expect further evolution to proceed according to (33) or (35). But, remarkably, these analytic results largely remain valid because the system *very quickly* recovers to the shape-preserving solution appropriate to the current value of N. This is most easily seen in Fig. 8, which illustrates the time evolution of the (normalized) terrace widths for an arbitrary initial profile by numerical solution of (30) and (31) for the case of diffusion-limited step propagation.

Additional interesting behavior during flattening is evident from the *velocity* of a "typical" terrace width depicted in Fig. 9. The nonanalytic spikes occurs each time N decreases and correspond to an impulsive "kick" felt by the terrace's bounding steps each time a contribution to the total step-step repulsion (18) is removed. After each spike, the velocity exhibits a short transient, whereupon $\dot{l}(t) \sim t^{-4/5}$, as expected from (33) for this case. We conclude that the shape-preserving solutions (33) and (35) behave, for each value of N, as *attractors* of the terrace equations of motion.

The actual appearance of the surface during the flattening described above is shown in Fig. 10. Each profile [again obtained by numerical solution of (30) and (31)] corresponds to a time immediately *after* a terrace annihilation has occured. Smooth curves have been drawn through points at the top of each step. Consistent with the foregoing, the initial (sinusoidal) surface rearranges considerably at the outset. Depending upon the precise starting shape, the system may or may not lose a few steps before it locks into the shape-preserving solution. Once this occurs, the currents across the terraces are indeed quite small near the extrema, increasing to a maximum at the inflection point of the profile. On the other hand, the step velocities—the difference between adja-

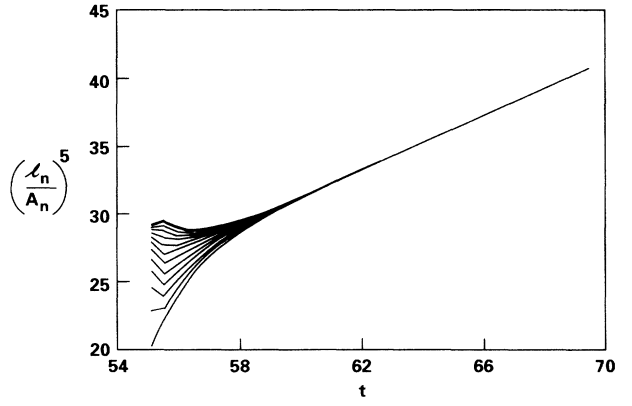

FIG. 8. Illustration that every terrace width (shown here for a case when 15 terraces are present) rapidly approaches the analytic solution (33) for the case of fast step-attachment kinetics. The depicted time interval begins immediately after a step has vanished and ends immediately before another step vanishes. Both scales are in arbitrary units.

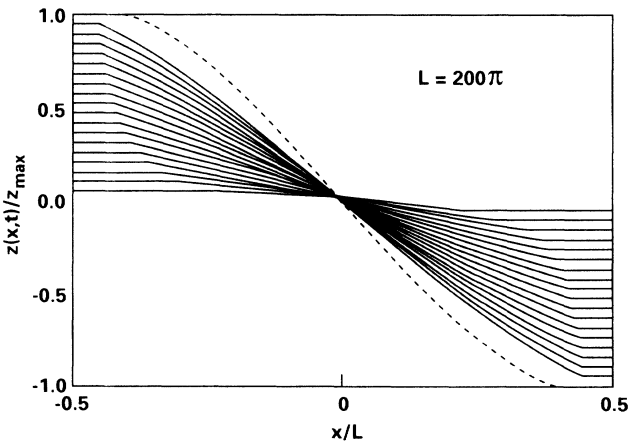

FIG. 10. Flattening of an initial sinusoidal profile (dashed curve) as determined by numerical solution of the discrete equations of motion (30).

cent currents (29)—are maximal near the extrema and minimal (zero) at the inflection point.

Unfortunately, we have been unable to derive an analytic expression for the time dependence of the profile amplitude directly from (33) or (35). Numerically, we find that $z^{-1}\sim t$ very nearly (Fig. 11). Although, again $z^{-1}\sim t^{1+\alpha}$ provides a rather better fit to the data—this time with $\alpha\simeq+0.025$. On the other hand, we can show easily that the amplitude function exhibits scaling behavior, i.e., $z(t)=F(t/L^5)$, where $2L$ is the period of the corrugation. To do so, it is necessary to suppose that the profile *always* exhibits a shape-preserving form, i.e., we ignore transients associated the initial conditions and presume that the profile instantaneously adopts the appropriate separated variable shape as N changes. As we have seen, the latter is not a bad approximation. Then, if t_N denotes the time required for the first set of extremal terraces to vanish for an N-step profile,

$$L=\sum_{n=1}^{N} l_n(t_N)=\sum_{n=1}^{N} A_n(N)\left[t_N+\left[\frac{l_n(0)}{A_n(N)}\right]^5\right]^{1/5} . \tag{40}$$

Now rescale all the initial terrace widths so that $l_n(0)\to\alpha l_n(0)$. In that case,

$$\begin{aligned} L'=\alpha L&=\sum_{n=1}^{N} l_n(t'_N)\\ &=\sum_{n=1}^{N} A_n(N)\left[t'_N+\left[\frac{\alpha l_n(0)}{A_n(N)}\right]^5\right]^{1/5} , \end{aligned} \tag{41}$$

which implies that $t'_N=\alpha^5 t_N$. The same argument applies for each time interval $T(N-2)$, $T(N-4)$, etc [with the appropriate quantities $A_n(N-2)$, $A_n(N-4)$, etc.]. This proves the assertion. One can show that the shape-preserving solution (13) to the continuum equation of motion exhibits the same scaling.

To truly complete our analysis, we ought to explicitly demonstrate how arbitrary initial conditions are drawn to the shape-preserving attractor. This appears to be a difficult task. However, we *can* show that *nearby* shapes evolve to this solution and thus provide some insight into the rapid decay of transients seen in Fig. 8. In what follows, we restrict ourselves to the case of fast kinetics; the corresponding analysis for slow kinetics proceeds similarly. Our strategy is to relax the requirement (37) and seek solutions to (30) of the form

$$l_n(t)=A_n[t+\bar{D}+f_n(t)]^{1/5} . \tag{42}$$

We make two assumptions: (i) $f_n(t)\ll t+\bar{D}$ at all times, and (ii) $f_n(t)\to 0$ smoothly as $t\to\infty$. Upon substitution, assumption (i) sanctions linearizing the resulting equations to

$$\dot{\mathbf{f}}=\frac{1}{t+\bar{D}}\mathbf{M}\cdot\mathbf{f}+\mathbf{R} , \tag{43}$$

where $\mathbf{f}$ is a column vector of the f_n, $\mathbf{R}$ is a column vector with components

$$R_n=\frac{5}{A_n}(K_{n+1}-2K_n+K_{n-1})-1 , \tag{44}$$

and $\mathbf{M}$ is an $N\times N$ banded matrix whose elements (simple functions of the A_n) are displayed explicitly in the Appendix. Assumption (ii) implies that $\mathbf{R}\to\mathbf{0}$ at large times. Comparing (44) with (38), this is seen to be equivalent to requiring that the A_n in (42) asymptotically approach those of the shape-preserving solution. But, since the A_n in our *ansatz* (42) are presumed to carry *no* time dependence, we must choose $\mathbf{R}=\mathbf{0}$ at *all* times.

The general solution to (43) (with $\mathbf{R}=0$) is

$$f_n(t)=\sum_{j=1}^{N}\xi_{nj}(t+\bar{D})^{\lambda_j} , \tag{45}$$

where λ_j are the eigenvalues[53] of $\mathbf{M}$ (not be be confused with the separation constant λ used earlier). The constants ξ_{nj} are determined by the initial conditions, while $\bar{D}$ is uniquely determined by assumption (ii). Numerically, we find that all $\lambda_j\le 0$ and are distinct. In particular, $\lambda_1=0$ always (for all N), while the other eigenvalues apparently converge to specific limiting values as the rank of $\mathbf{M}$ increases. Thus, $\lambda_2=-5$ (converged at $N=9$), $\lambda_3=-25$ (converged at $N=12$), etc. These large values for $|\lambda_j|$ make clear why $l_n(t)\sim A_n t^{1/5}$ very rapidly even if the initial terrace widths do not satisfy (37). One can verify that the constant $\bar{D}$ emerges as a weighted average of these widths,

$$\bar{D}=\sum_{k=1}^{N}\eta_k\left[\frac{l_k(0)}{A_k}\right]^5 , \tag{46}$$

where the constants η_k depend upon N.

The utility of this analysis can be judged from Fig. 12, which compares $l_1(t)$ and $\dot{l}_1(t)$ as obtained by an exact numerical solution of (30) (in the fast-kinetics limit) with the predictions of (42) for several different surface profiles. In each case, $l_1(0)$ deviates from (37) by the indicated percentages. Although the analytic results are surprisingly good, even better agreement would be obtained if one admitted time-dependent amplitudes $A_n(t)$ into the perturbation theory.

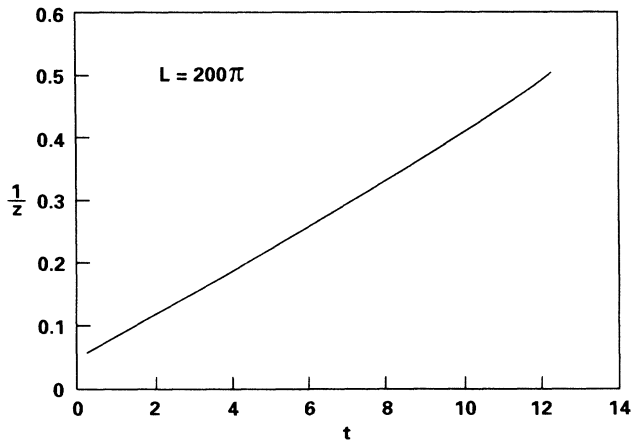

FIG. 11. Inverse profile amplitude vs time (both in arbitrary units) for the flattening sequence of Fig. 10.

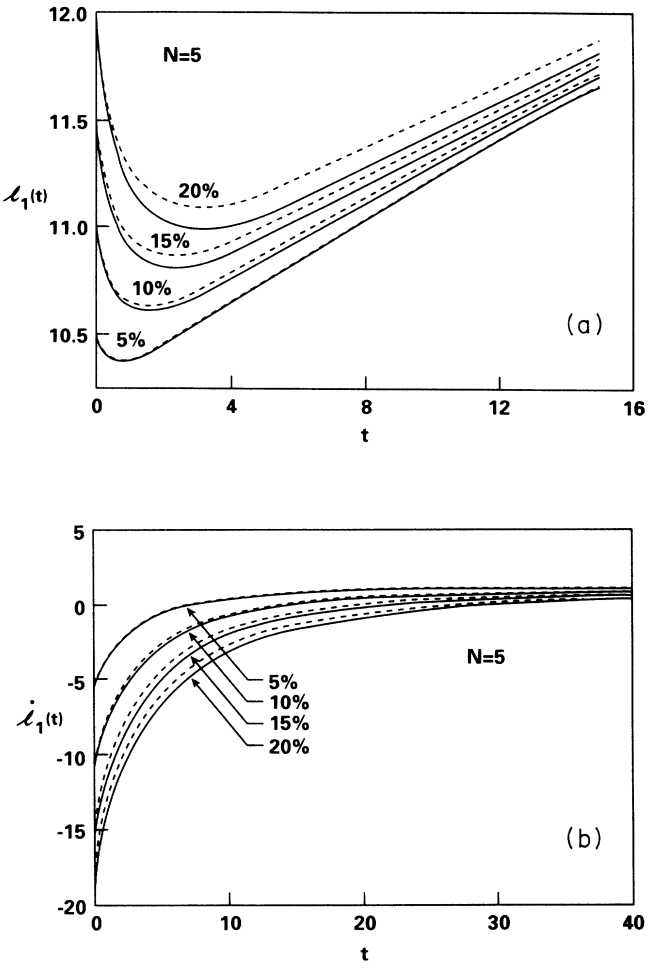

FIG. 12. (a) time evolution of $l_1(t)$ and (b) $\dot{l}_1(t)$ as determined from (30) numerically (solid curves) and from the approximate analytic solution (42) (dashed curves) for cases when $l_1(0)$ deviates from (37) by the indicated percentages.

Finally, as promised, let us return to the situation where l_n and d are of comparable magnitude, so that neither of the limiting forms (33) or (36) is appropriate. The discrete equations of motion (30) then are quite formidable—except when $N=1$. In that case, the problem is integrable and (denoting the single nonextremal terrace width by l) one finds

$$\frac{1}{4}\left[\frac{l(t)}{d}\right]^4+\frac{1}{5}\left[\frac{l(t)}{d}\right]^5=\left[\frac{4B_4}{d^5}\right]t+D\ , \tag{47}$$

where $D=\frac{1}{4}[l(0)/d]^4+\frac{1}{5}[l(0)/d]^5$. We speculate that the crossover from diffusion-limited to step-attachment-limited step motion is not very different from this even when $N\neq 1$.

V. DISCUSSION

Generally speaking, good correspondence is found between the results obtained from the continuum theory of the surface profile alone (Sec. II) and those obtained from the more complete account of the motion of individual steps (Sec. IV). This is clear from a comparison of the flattening sequences shown in Figs. 2 and 10, which both correspond to sinusoidal initial conditions. Moreover, both approaches yield $z^{-1}\simeq t$ and predict identical nonanalytic behavior of the shape-preserving solution near local extrema. These results imply that one ought to be able to derive (10) from (32) in a suitable continuum limit [despite the fact that our numerical solution of (10) did not produce shape-preserving evolution]. Unfortunately, in the step picture, the profile amplitude decreases discontinuously whenever approaching steps collide and annihilate. Since the times when these collisions occur are unknown at the outset, it appears difficult to make a general correspondence between the $\dot{l}_n(t)$ and $\dot{z}(t)$.

On the other hand, consider a comparison of the two approaches for a case where the starting profile differs substantially from a sinusoid (Fig. 13). Now, although both dynamics inexorably lead to flattening as time goes on, an interesting difference appears in the initial transient period. In the continuum case, an energetically costly region of high curvature is quickly removed by transfer of mass to the top of the profile. Hence, the am-

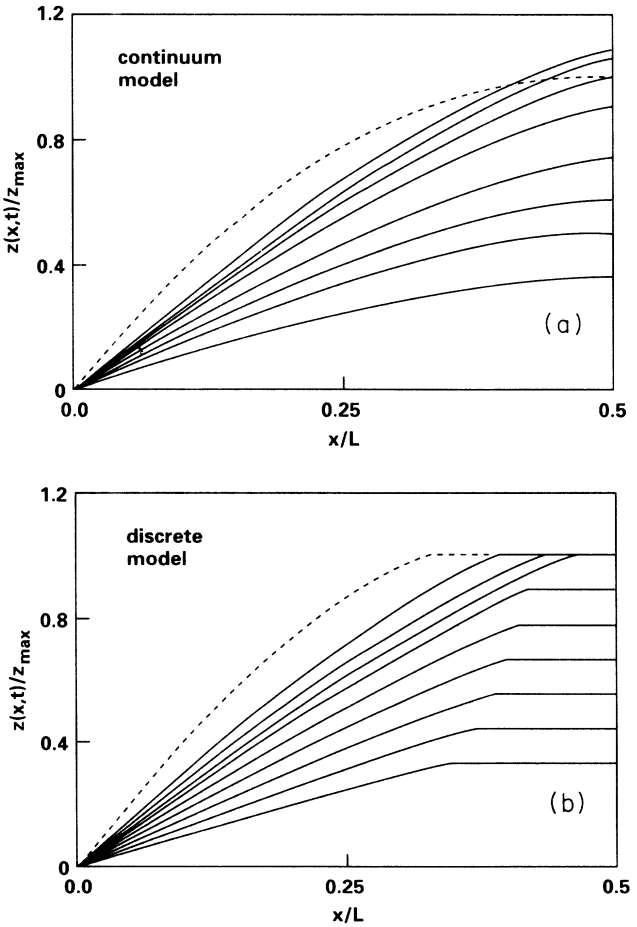

FIG. 13. Morphological equilibration of an initial profile (dashed curve) which differs substantially from a sinusoid as determined numerically from the (a) continuum theory and (b) the discrete step theory. For the latter, some of the transient behavior of the top terrace (before even the first pair of steps vanish) is shown for comparison.

plitude of the corrugation wave *increases* at first before flattening proceeds. In the discrete case, no such increase occurs and, in fact, is explicitly forbidden because we permit no increase in the number of steps or (equivalently) the number of coupled equations of motion (30). Although *formally* one could allow for this effect, it would be incorrect to do so since no account is thereby taken of the (considerable) nucleation barrier to the formation of a new layer. By contrast, the continuum equation blithely pushes mass onto the top of the profile. In this sense, the discrete equations probably provide a better account of the initial transient period.

In agreement with previous work,[14] we find that no facets form during flattening. On the other hand, facets definitely are observed under some experimental conditions.[21,41] Villain and Lançon[28] have suggested that this can occur only if the original "flat" crystal is, in fact, slightly *miscut* in the direction perpendicular to the direction of corrugation. Taking this into account, they derive continuum equations of motion formally equivalent to those employed (phenomenologically) in Ref. 41. As stated, this result appears to depend crucially on the presence of curved terrace edges at the extrema of the profile (see Fig. 2 of Ref. 30) so that there exists a line-tension contribution to the driving force for morphological evolution. If, however, there is appreciable in-plane anisotropy (as should be expected even above the step-roughening temperature), all terrace edges will be nearly straight (apart from thermal wandering) and only step-step repulsion (18) will be operative as in the case considered here. In particular, step velocities parallel and perpendicular to the direction of corrugation will be comparable in magnitude. No facets should form. Investigation of this issue clearly warrants further systematic experimental investigation.

Two important caveats remain. The first involves our assumption that there is no interaction between pairs of "unlike" steps which bound terraces at the extrema of the surface profile. Although an attractive force would merely accelerate flattening, a repulsive force (depending upon its nature) certainly would retard this process. Evidently, the existence of such a force would determine in detail the nature of the annihilation of extremal terraces. Even in the absence of interaction, our treatment of this feature is qualitative at best. Entropy driven formation of closed loops at these moments has been predicted[14] and apparently observed by simulation.[35]

Second, we remind the reader that the foregoing implicitly assumes that the initial corrugation wave is of rather small amplitude. This restriction enters our calculations at a number of places, but most particularly in the expansion of the surface free energy in Eqs. (8) and (18). No allowance is taken of the possible metastability of facets with orientation at finite angles from the horizontal. This surely must be relevant for discussion of the annealing properties of corrugated semiconductor surfaces fabricated with pitch and amplitude of similar magnitude[54] or of those explicitly designed to expose inequivalent crystallographic facets.[15,16] Work along these lines is in progress and will be reported elsewhere.

VI. SUMMARY

In this paper, we have studied morphological equilibration via surface diffusion of a (small amplitude) corrugated surface below its roughening temperature. For the considered geometry, the problem is one-dimensional and step motion is driven by step-step interactions only. The dynamics turn out to be highly nonlinear. As evolution proceeds, all terraces' widths $l_n(t)$ ultimately expand except those that correspond to local maxima and minima of the surface profile $z(x,t)$. A central result is that an arbitrary profile flattens via step motion as one would predict on the basis of the separated variable solution to the discrete equations of motion. In particular, $l_n(t)\sim t^{1/5}$ or $l_n(t)\sim t^{1/4}$ (depending upon the relative importance of surface diffusion and step-attachment kinetics) and $z(x,t)\sim t^{-1}$ apart from transients. No facets form if equilibrium corresponds to a perfectly flat surface. Thus, for those experimental systems where flattening occurs *without* faceting, yet $T<T_R$, our predictions should be valid and testable by, e.g., *in situ* reflection high-energy electron microscopy.[9]

ACKNOWLEDGMENTS

We have benefited from conversations with Ron Fox, Gunter Meyer, Kurt Wiesenfeld, and, most particularly, from a lively correspondence with Jacques Villain. The authors gratefully acknowledge support for this work under U.S. Department of Energy Grant No. DE-FG05-88ER45369.

APPENDIX

The banded matrix $\underline{M}$ which appears in Sec. IV has the form

$$\begin{pmatrix}
M_{11} & M_{12} & M_{13} & 0 & 0 & 0 & & & \\
M_{21} & M_{22} & M_{23} & M_{24} & 0 & 0 & & 0 & \\
M_{31} & M_{32} & M_{33} & M_{34} & M_{35} & 0 & & & \\
0 & M_{42} & M_{43} & M_{44} & M_{45} & M_{46} & & & \\
 & & & & \ddots & & & & \\
 & & & M_{N-3,N-5} & M_{N-3,N-4} & M_{N-3,N-3} & M_{N-3,N-2} & M_{N-3,N-1} & 0 \\
 & & & 0 & M_{N-2,N-4} & M_{N-2,N-3} & M_{N-2,N-2} & M_{N-2,N-1} & M_{N-2,N} \\
 & 0 & & 0 & 0 & M_{N-1,N-3} & M_{N-1,N-2} & M_{N-1,N-1} & M_{N-1,N} \\
 & & & 0 & 0 & 0 & M_{N,N-2} & M_{N,N-1} & M_{N,N}
\end{pmatrix}.$$

The matrix elements depend only on the quantities A_n [defined in (38)] and hence reflect the symmetry seen in Fig. 6. In particular, one has

$$M_{ij}=M_{|N-i+1|,\,|N-j+1|}$$

so that all nonzero elements can be found from

$$M_{11}=\frac{1}{A_1}\left[\frac{2}{A_1}\left[\frac{1}{A_2^3}-\frac{2}{A_1^3}\right]-\frac{3}{A_1^3}\left[\frac{1}{A_2}+\frac{4}{A_1}\right]+\tfrac{4}{5}A_1\right],$$

$$M_{12}=\frac{1}{A_1}\left[\frac{6}{A_2^3}\left[\frac{1}{A_2}+\frac{1}{A_1}\right]-\frac{1}{A_2}\left[\frac{1}{A_3^3}-\frac{2}{A_2^3}+\frac{1}{A_1^3}\right]\right],$$

$$M_{13}=-\frac{3}{A_3^3}\frac{1}{A_2}\frac{1}{A_1},$$

$$M_{21}=\frac{1}{A_2}\left[\frac{6}{A_1^3}\left[\frac{1}{A_2}+\frac{1}{A_1}\right]-\frac{1}{A_1}\left[\frac{1}{A_2^3}-\frac{2}{A_1^3}\right]\right],$$

$$M_{22}=\frac{1}{A_2}\left[\frac{2}{A_2}\left[\frac{1}{A_3^3}-\frac{2}{A_2^3}+\frac{1}{A_3^3}\right]-\frac{3}{A_2^3}\left[\frac{1}{A_3}+\frac{4}{A_2}+\frac{1}{A_1}\right]+\tfrac{4}{5}A_2\right],$$

$$M_{23}=\frac{1}{A_2}\left[\frac{6}{A_3^3}\left[\frac{1}{A_3}+\frac{1}{A_2}\right]-\frac{1}{A_3}\left[\frac{1}{A_4^3}-\frac{2}{A_3^3}+\frac{1}{A_2^3}\right]\right],$$

$$M_{24}=-\frac{3}{A_4^3}\frac{1}{A_3}\frac{1}{A_2},$$

and, for $3\le n\le N-2$,

$$M_{n,n-2}=-\frac{3}{A_{n-2}^3}\frac{1}{A_{n-1}}\frac{1}{A_n},$$

$$M_{n,n-1}=\frac{1}{A_n}\left[\frac{6}{A_{n-1}^3}\left[\frac{1}{A_n}+\frac{1}{A_{n-1}}\right]-\frac{1}{A_{n-1}}\left[\frac{1}{A_n^3}-\frac{2}{A_{n-1}^3}+\frac{1}{A_{n-2}^3}\right]\right],$$

$$M_{n,n}=\frac{1}{A_n}\left[\frac{2}{A_n}\left[\frac{1}{A_{n+1}^3}-\frac{2}{A_n^3}+\frac{1}{A_{n-1}^3}\right]-\frac{3}{A_n^3}\left[\frac{1}{A_{n+1}}+\frac{4}{A_n}+\frac{1}{A_{n-1}}\right]+\tfrac{4}{5}A_n\right],$$

$$M_{n,n+1}=\frac{1}{A_n}\left[\frac{6}{A_{n+1}^3}\left[\frac{1}{A_{n+1}}+\frac{1}{A_n}\right]-\frac{1}{A_{n+1}}\left[\frac{1}{A_{n+2}^3}-\frac{2}{A_{n+1}^3}+\frac{1}{A_n^3}\right]\right],$$

$$M_{n,n+2}=-\frac{3}{A_{n+2}^3}\frac{1}{A_{n+1}}\frac{1}{A_n}.$$

[1] E. H. C. Parker, *The Technology and Physics of Molecular Beam Epitaxy* (Plenum, New York, 1985).

[2] G. B. Stringfellow, *Organometallic Vapor Phase Epitaxy* (Academic, New York, 1989).

[3] H. Yamaguchi, M. Kawashima, and Y. Horikoshi, Appl. Surf. Sci. **33-34**, 406 (1988).

[4] C. H. L. Goodman and M. V. Pessa, J. Appl. Phys. **60**, R65 (1986).

[5] J. A. Venables, T. Doust, and R. Kariotis, in *Initial Stages of Epitaxial Growth*, edited by R. Hull, J. M. Gibson, and D. A. Smith (Materials Research Society, Pittsburgh, 1987), pp. 3–14.

[6] S. Stoyanov and M. Michailov, Surf. Sci. **202**, 109 (1988).

[7] R. Kariotis and M. G. Lagally, Surf. Sci. **216**, 557 (1989).

[8] S. Clarke, M. R. Wilby, D. D. Vvedensky, and T. Kawamura, Phys. Rev. B **40**, 1369 (1989).

[9] P. K. Larsen and P. J. Dobson, *Reflection High Energy Electron Diffraction and Reflection Electron Imaging of Surfaces* (Plenum, New York, 1988).

[10] E. Bauer, M. Mundschau, W. Swiech, and W. Telieps, Ultramicrosc. **31**, 49 (1989).

[11] E. Chason, J. Y. Tsao, K. M. Horn, and S. T. Picraux, J. Vac. Sci. Technol. B **7**, 332 (1989).

[12] H. Kahata and K. Yagi, Jpn. J. Appl. Phys. Pt. 2 **28**, L858 (1989).

[13] H. P. Bonzel, N. Freyer, and E. Preuss, Phys. Rev. Lett. **57**, 1024 (1986).

[14] A. Rettori and J. Villain, J. Phys. (Paris) **49**, 257 (1988).

[15] H. Nagai, Y. Noguchi, and T. Matsuoka, J. Cryst. Growth **71**, 225 (1985).

[16]Z. L. Liau and H. J. Zeiger, J. Appl. Phys. **67**, 2434 (1990).
[17]W. W. Mullins, J. Appl. Phys. **30**, 77 (1959).
[18]W. W. Mullins, in *Metal Surfaces,* edited by W. D. Robertson and N. A. Gjostein (American Society for Metals, Metals Park, OH, 1963), pp. 17–66.
[19]J. M. Blakely and H. Mykura, Acta Metall. **1D**, 565 (1962).
[20]J. M. Blakely and C. C. Umbach, in *Diffusion at Interfaces: Microscopic Concepts,* edited by M. Grunze, H. J. Kreuzer, and J. J. Weimer (Springer, Berlin, 1988), pp. 102–110.
[21]H. P. Bonzel, in *Surface Mobilities on Solid Materials,* edited by V. T. Binh (Plenum, New York, 1983), pp. 195–218.
[22]C. Herring, Phys. Rev. **82**, 87 (1951).
[23]M. Wortis, in *Fundamental Problems in Statistical Mechanics VI,* edited by E. G. D. Cohen (North-Holland, Amsterdam, 1985), pp. 87–123.
[24]Ya. E. Geguzin and N. N. Ovcharenko, Kristaliografiya **7**, 1 (1961) [Sov. Phys.—Crystallogr. **6**, 75 (1961)].
[25]G. Martin and B. Perraillon, Surf. Sci. **68**, 57 (1977).
[26]M. Uwaha, J. Phys. Soc. Jpn. **57**, 1681 (1988).
[27]J. Villain, Europhys. Lett. **2**, 531 (1986).
[28]J. Villain and F. Lançon, C. R. Acad. Sci. Paris **309**, Ser. II, 647 (1989).
[29]F. Lançon and J. Villain, in *Kinetics of Ordering and Growth at Surfaces,* edited by M. Lagally (Plenum, New York, 1990).
[30]F. Lançon and J. Villain, Phys. Rev. Lett. **64**, 293 (1990).
[31]H. van Beijeren and I. Nolden, in *Structure and Dynamics of Surfaces II,* edited by W. Schommers and P. von Blanckenhagen (Springer, Berlin, 1987), pp. 259–300.
[32]D. W. Hoffman and J. W. Cahn, Surf. Sci. **31**, 368 (1972); J. W. Cahn and D. W. Hoffman, Acta Metall. **22**, 1205 (1974).
[33]J. Villain, C. R. Acad. Sci. Paris **309**, Ser. II, 517 (1989).
[34]See, e.g., M. Ohara and R. C. Reid, *Modelling Crystal Growth Rates from Solution* (Prentice-Hall, Englewood Cliffs, NJ, 1973).
[35]W. Selke and J. Oitmaa, Surf. Sci. **198**, L346 (1988).
[36]Z. Jiang and C. Ebner, Phys. Rev. B **40**, 316 (1989).
[37]J. Villain (private communication).
[38]C. Herring, in *The Physics of Powder Metallurgy,* edited by W. E. Kingston (McGraw-Hill, New York, 1951), pp. 143–179.
[39]J. J. Saenz and N. Garcia, Surf. Sci. **155**, 24 (1985).
[40]J. J. Metois and J. C. Heyraud, Surf. Sci. **180**, 647 (1987).
[41]E. Preuss, N. Freyer, and H. P. Bonzel, Appl. Phys. A **41**, 137 (1986), and references therein.
[42]W. K. Burton, N. Cabrera, and F. C. Frank, Philos. Trans. R. Soc. London, Ser. A **243**, 299 (1951).
[43]M. Uwaha and P. Nozières, in *Morphology and Growth Unit of Crystals,* edited by I. Sunagawa (Terra Scientific, Tokyo, 1989).
[44]P. Nozières, J. Phys. (Paris) **48**, 1605 (1987).
[45]R. Ghez and S. S. Iyer, IBM J. Res. Dev. **32**, 804 (1988).
[46]N. Cabrera, Surf. Sci. **2**, 320 (1964).
[47]A. F. Andreev and Yu. A. Kosevich, Zh. Eksp. Teor. Fiz. **81**, 1435 (1981) [Sov. Phys.—JETP **54**, 761 (1981)].
[48]E. M. Pearson, T. Halicioglu, and W. A. Tiller, Surf. Sci. **184**, 401 (1987).
[49]E. E. Gruber and W. W. Mullins, J. Phys. Chem. Solids **28**, 875 (1967).
[50]In fact, according to Ref. 47, pairs of "unlike" steps, e.g., those which bound terraces at local extrema of the surface profile, can exert either a repulsive or an attractive force on one another, depending upon the elastic properties of the underlying solid.
[51]R. Ghez, *A Primer of Diffusion Problems* (Wiley, New York, 1988).
[52]R. H. Doremus, *Rates of Phase Transformations* (Academic, New York, 1985).
[53]Equation (45) is a solution to (43) only if the eigenvalues of the matrix $\underline{M}$ are all distinct. This turns out to be the case.
[54]E. Inamura, Y. Miyamoto, S. Tamura, T. Takasugi, and K. Furuya, Jpn. J. Appl. Phys. Pt. 2 **28**, 2193 (1989).